JOURNAL OF PROPULSION AND POWER
Vol. 17, No. 5, September–October 2001

Technical Notes

TECHNICAL NOTES are short manuscripts describing new developments or important results of a preliminary nature. These Notes cannot exceed 6 manuscript pages and 3 figures; a page of text may be substituted for a figure and vice versa. After informal review by the editors, they may be published within a few months of the date of receipt. Style requirements are the same as for regular contributions (see inside back cover).

Mixing of Supersonic Jets in a Strutjet Propulsion System

S. Muller*
Delft University of Technology, Delft, The Netherlands 2629 HS
Clark W. Hawk†
University of Alabama in Huntsville, Huntsville, Alabama 35899
P. G. Bakker‡
Delft University of Technology, Delft, The Netherlands 2629 HS
and
D. Parkinson,§ and M. Turner¶
University of Alabama in Huntsville, Huntsville, Alabama 35899

Introduction

A SCALE model of the strutjet device for a rocket-based combined cycle (RBCC) was built and tested to investigate the mixing of the streams as a function of distance from the strut exit plane in simulated sea-level takeoff conditions. The planar laser–induced fluorescence (PLIF) diagnostic method was employed to observe the mixing of the simulated turbine exhaust gas with the gases from both the primary rockets and the ingested air. The ratio of the pressure in the turbine exhaust to that in the rocket nozzle wall at the point of their intersection was the independent variable in these experiments. Tests were accomplished at values of 1.0 (the original design point), 1.5, and 2.0 for this parameter, and images of the degree of mixing were taken at eight locations downstream of the nozzle exit plane. The results illustrate the development of the mixing zone from the exit plane of the strut to a distance of about 18 equivalent rocket nozzle exit diameters downstream (45.72 cm). These images show the mixing to be confined until a short distance downstream of the nozzle for a single nozzle geometry set. The lateral expansion is more pronounced at pressure ratios of 1.0 and 1.5, indicating that mixing with the ingested airflow would be likely to begin at an L/D of approximately 1 downstream of the nozzle exit plane. Of the pressure ratios tested in this research, a value of 2.0 delays the mixing until an L/D of approximately 2 and was the best value at the operating conditions considered.

This research effort focused on the mixing behavior of rocket and turbine exhaust jets in the RBCC strutjet concept during a simulated sea-level takeoff condition. The strutjet propulsion concept is designed to operate in four different modes: ducted rocket or air-augmented mode, ramjet mode, scramjet mode, and a pure rocket mode.[1] The strutjet approach to RBCC propulsion depends upon fuel-rich flows from the rocket nozzles and turbine exhaust products mixing with the ingested air for successful operation in the ramjet and scramjet modes.

In the air-augmented rocket mode that is of interest here, the mixing of the fuel-rich turbine exhaust with the ingested air should be delayed to prevent thermal choking in the expansion section of the engine. The nozzle arrangement investigated in this research was designed to achieve this end by injecting the turbine exhaust between the rocket plumes to shield the fuel-rich turbine exhaust from the ingested air and delay the heat release. This configuration was intended to promote mixing in the vertical direction (among the turbine and rocket exhausts) before they mix with the ingested air. The goal of this research was to determine the effectiveness of the chosen geometry in delaying mixing with the ingested air in the air-augmented mode of operation.

Experimental Setup

Flow Section

This research was done with a $\frac{1}{6}$th-scale model of one strut equipped with two simulated rocket exhausts flowing heated air and one simulated turbine exhaust between them, flowing heated CO_2 (Fig. 1). The area ratio of the rocket nozzles is 4.65 and the turbine nozzle is 1.184. The turbine exhaust plane is located upstream of the rocket exhaust plane (Fig. 2). The flow from the turbine intersects

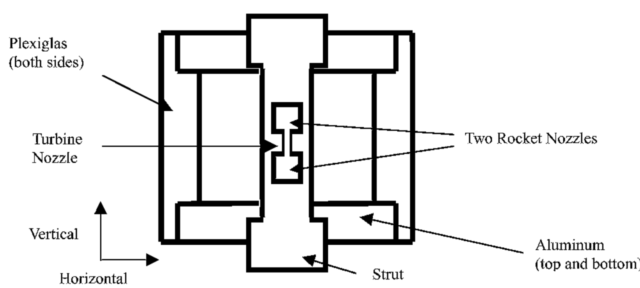

Fig. 1 Test configuration.

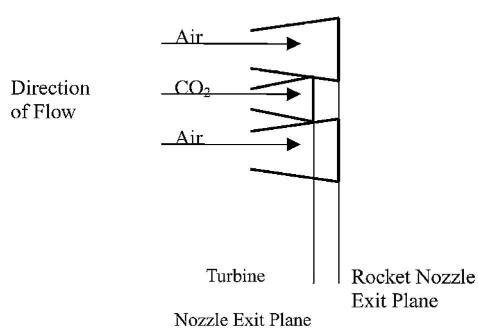

Fig. 2 Nozzle configuration.

Received 7 August 2000; revision received 1 March 2001; accepted for publication 30 April 2001.

*Student, Faculty of Aerospace Engineering; currently Sverdrup Technology, Advanced Technology Segment. Member AIAA.

†Professor, Faculty of Aerospace Engineering.

‡Professor, Mechanical and Aerospace Engineering, and Director, Propulsion Research Center. Fellow AIAA.

§Student, Department of Mechanical and Aerospace Engineering; currently Marshall Space Flight Center (NASA). Member AIAA.

¶Student, Department of Mechanical and Aerospace Engineering. Member AIAA.

the rocket flow upstream of the rocket nozzle exit plane. At this location, the area ratio of the rocket nozzle is 2.99. The design chamber pressures were chosen such that the turbine exhaust intersects the rocket flow where each has the same local pressure. We also tested the influence of the pressure ratio ($p_{\text{turbine}}/p_{\text{rocket}}$) of the exhaust gases at the point of contact, performing the measurements at three values of the ratio, 1.0, 1.5, and 2.0.

We chose a similarity parameter of convective Mach number as a means to achieve the same mixing behavior in the scaled experiment as in a representative size system. Papamoschou and Roshko[2] experimentally found this similarity parameter for supersonic shear layer growth rates. A convective Mach number of 0.6, determined for each test at the point where the two flows intersected, was chosen for the experiments as representative of the full-scale engine.[3] The choice of modeling parameter dictated the selection of many of the independent variables in the experiments.

We selected PLIF as the diagnostic technique. The turbine flow was simulated using CO_2 gas. It was supplied to the model at a mass flow rate of 4.54×10^{-2} kg/s and 6.12 atm. Laboratory-grade acetone was introduced as the seedant upstream of the model. The seedant was kept at a constant molar fraction of 11%. The CO_2 gas was heated to 422 K stagnation temperature to prevent acetone from condensing in the nozzle.

Both the rocket nozzle flow and the turbine flow required the same stagnation temperature to maintain the convective Mach number at 0.6. An airflow of 0.91 kg/s was delivered to each rocket nozzle at 422 K and a total pressure of up to 51 atm.

The model was placed in a rectangular duct (about 4×4 in. cross-section) with an aluminum top and bottom and transparent sidewalls (Fig. 1). The sidewalls are modular, with interchangeable sections, to allow easy access to the model and permit direct observation of the flow. The duct has a two-dimensional bellmouth inlet open to the atmosphere, providing a smooth ingested airflow. The assembly discharges the flow into free air through a 10-in.-diam duct.[4]

Diagnostics

The PLIF diagnostic method was used to visualize the mixing of the gas flows. This involved exciting the acetone with UV radiation at a wavelength of 266 nm provided by a frequency-quadrupled Spectra-Physics Quanta-Ray GCR290 Nd:YAG laser, emitting pulses of 10 ns at a rate of 10 Hz. The UV beam was made into a laser sheet 8.89 cm high and about 500 μm thick by means of a convex and a cylindrical lens and guided to the test location. The imaging location was positioned axially along the duct by moving the last prism and the two lenses (Fig. 3).

Sections of the duct sidewall on the laser side were fit with a fused silica window (8.89×8.89 cm) to permit minimal loss of the beam energy before encountering the flowing gases. These special sections were located at axial locations from the nozzle exit plane to 22.9 cm downstream and 45.7 cm downstream of the nozzle exit plane. The excited acetone vapor fluoresces, emitting broadband radiation at wavelengths between 300 and 700 nm. The fluorescent signal was collected over a bandwidth of 300–495 nm to eliminate interference from scattered 266 and 532 nm laser light. This range of wavelengths accounts for about 80% of the fluorescence radiation energy, ensuring that a signal of sufficient strength is available for collection.[5] The opposite side of the duct consisted of a single piece of Plexiglas® mounted to allow an unobstructed view for the camera. This sidewall will absorb the remainder of the UV radiation, and a visible short pass (VSP) filter in front of the camera absorbs light with a wavelength over 495 nm. Finally, the signal was collected by a Princeton Instruments ICCD camera.

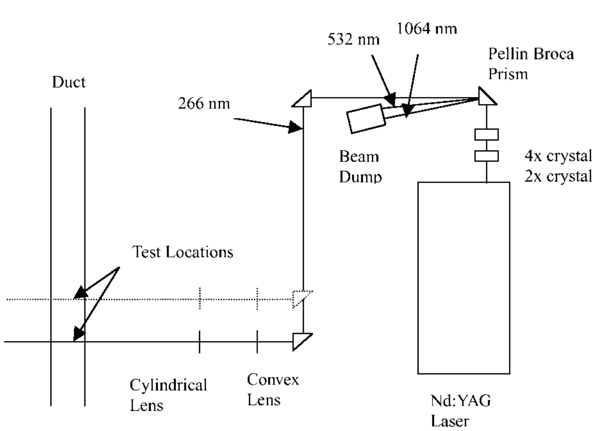

Fig. 3 Laser setup.

Acetone fluorescence has a lifetime of less than 4 ns. Acetone also phosphoresces at wavelengths similar to the fluorescence, albeit at a much greater lifetime of about 200 μs. The phosphorescence interference was rendered negligible by gating the intensified camera around the laser pulse (10 ns) at 13 ns. This also eliminated interference from surrounding light sources.

Experimentation

Tests were performed for the three pressure ratios (1.0, 1.5, and 2.0) between the rocket and turbine nozzles. With the chamber pressure of the turbine nozzle maintained at 6.67 ± 0.34 atm, the rocket chamber pressures were set to 37.4, 24.9, and 18.7 atm, respectively, to achieve these pressure ratios. The pressure at the point of intersection for these operating conditions yielded 1.78 atm in the turbine exhaust and 1.78, 1.18, and 0.89 atm, respectively, in the rocket nozzle.

Fluorescent Signal

Fluorescence from acetone for weak excitation can be modeled by the following relationship, showing the wavelength and temperature dependencies[6]:

$$(\lambda, T) = \eta_{\text{opt}}[E/(hc/\lambda)]\,\mathrm{d}V_c n_{\text{abs}}(T)\sigma(\lambda, T)\phi(\lambda, T)$$

where S_f is the intensity of the fluorescence, η_{opt} is the overall efficiency of the collection optics, E is the laser fluence (J/cm^2), (hc/λ) is the energy (J) of a photon at excitation wavelength λ, and $\mathrm{d}V_c$ is the collection volume (cm^3). The temperature-dependent quantities are n_{abs}, the number density of absorbing molecules (cm^{-3}); σ, the molecular absorption cross-section of the tracer (cm^2); and ϕ, the fluorescence quantum yield.

Because the optical setup is the same for all tests performed, the overall efficiency of the collection optics, η_{opt}, was assumed to be constant. The laser fluence, E, was also assumed to be a constant, because the laser energy was monitored and kept at the same level for all tests and the dimensions of the laser sheet entering the test section were constant. The energy of the photons (hc/λ) depends only on the wavelength of the laser light and is therefore also constant. The term $\sigma(\lambda, T)\ \phi(\lambda, T)$ [defined as $S_f^*(\lambda, T)$] has a relatively small dependency on temperature for the range expected to occur in the experiment. The maximum variation is about 10% for the temperature range (300–450 K) of the experiment. The term $\mathrm{d}V_c n_{\text{abs}}$ is equal to the number of tracer molecules hit by the laser. Because the laser sheet had the same dimensions for all tests, this term is proportional to the density of the acetone in the CO_2, and because the molar fraction of the seeding is constant, the term is also proportional to the density of the entire simulated turbine flow.

This implies that if there is a variation greater than 10% in the fluorescence signal, this must be due to a variation in the density of the acetone in the turbine flow. This density change can be caused by an event like a shock or expansion wave, which does not necessarily mean that mixing has taken place. Therefore the images were normalized to the total fluorescence signal of the picture. This provides a picture that shows the percentage of acetone molecules hit by the laser within each pixel of the image. High values in an image will then indicate the presence of a concentrated core flow, and low values will show that the turbine flow has spread out.

Processing of the Images

One image that was considered most representative of the run was retained from each test run. The software from Princeton

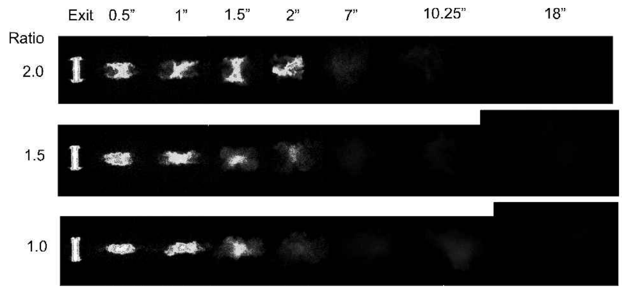

Fig. 4 Normalized images of the mixing.

Instruments (WinView 1.6.2) used to operate the camera was also used for further processing of the images. The background reflections were removed by subtraction, then the images were normalized to the total fluorescence signal. All the negative values in the image, caused by small differences between the background image and the background of the fluorescence image, were first set to 0 to further reduce the influence of the background. The total signal was then determined by adding the values of all the pixels with a value of over 10% of the maximum value in the image. The threshold was set at 10% to minimize the contribution of the background to the total.

Results

The resulting images can be seen in Fig. 4. These images have been resized to the same scale to enable comparisons of the turbine flow distribution. The pressure ratio ($p_{\text{turbine}}/p_{\text{rocket}}$) for each test is shown on the left and the image locations are measured from the exit plane of the strut.

In all cases, the conditions at the exit plane are quite similar. The turbine flow is clearly expanding into the rocket nozzles, forming a shape best described by the letter "I." At a pressure ratio of 1.0, the turbine nozzle flow is compressed vertically and experiences a strong lateral expansion. The flow appears almost completely dispersed at a distance of 5.1 cm. As the pressure ratio increased, the vertical expansion of the turbine flow (in the plane of the nozzle wall divergence) appears enhanced. The greater the pressure ratio, the greater the lateral expansion at the top and bottom of the "I," where the simulated rocket and turbine flows intersect. This lateral expansion of the turbine flow appears better defined, in general, for the pressure ratio 2.0 case and remains more or less intact to a distance of at least 5.1 cm downstream. The pressure differential would appear to be initiating a vortex flow at the point of intersection with the rocket nozzle flow. In all cases, the turbine flow is virtually dissipated by the time it reaches the 17.8 cm downstream location, but the higher the pressure ratio, the less the dispersion of the turbine flow into the surrounding nozzle and ingested air flows.

Conclusions

The operating pressure ratio ($p_{\text{turbine}}/p_{\text{rocket}}$) had a measurable effect on delaying the mixing distance for the one specific configuration of the rocket and turbine exhaust nozzles tested. The turbine exhaust gas exhibited increasingly well-defined confinement of the core flow and greater distance required until full dispersion of the exhaust was realized as the pressure ratio was increased from 1.0 to 2.0. This may be explained by either of two phenomena: 1) Because the rocket nozzle pressure was controlled by the plenum pressure, the nozzle mass flow rates varied inversely with the pressure ratio between the turbine exhaust and the rocket. Because the nozzle pressure ratios (stagnation to the pressure at the point of intersection) remained constant and the static temperature of the flows was held constant, the momentum of the nozzle flow also decreased in direct proportion to the increase in the pressure ratios. Consequently, the greater momentum of the nozzle flow in the case where pressure ratio equals 1.0 serves to confine the vertical expansion of the turbine flow, with consequent increased lateral expansion and more rapid dissipation. 2) The vortex flow initiated where the flows intersect may play a role in containing the central flow of the turbine flow to a greater distance downstream than is the case for the pressure ratio of one.

Acknowledgments

This research was accomplished under cooperative agreement NCC8-123 with NASA/Marshall Space Flight Center. The authors gratefully acknowledge the advice and counsel of Mike Fazah of NASA/Marshall Space Flight Center and Larry Cohen of GenCorp Aerojet, and the encouragement of Uwe Hueter of NASA/Marshall Space Flight Center.

References

[1] Siebenhaar, A., and Bulman, M. J., "The Strutjet Engine: The Overlooked Option for Space Launch," AIAA Paper 95-3124, July 1995.

[2] Papamoschou, D., and Roshko, A., "The Compressible Turbulent Shear Layer: An Experimental Study," *Journal of Fluid Mechanics*, Vol. 197, 1998, pp. 453–477.

[3] Spetman, D. M., Hawk, C. W., and Moser, M. D., "Development of a Strutjet Cold-Flow Mixing Experiment," *Journal of Propulsion and Power*, Vol. 15, No. 1, 1999, pp. 155–158.

[4] Parkinson, D., Turner, M., and Wagner, D., "Mixing of Hypersonic Streams," AIAA Paper 99-2454, June 1999.

[5] Thurber, M. C., Grisch, F., Kirby, J. K., Votsmeier, M., and Hanson, R. K., "Measurements and Modeling of Acetone Laser-Induced Fluorescence with Implications for Temperature-Imaging Diagnostics," *Applied Optics*, Vol. 37, No. 21, 1998, pp. 4963–4978.

[6] Lozano, A., Yip, B., and Hanson, R. K., "Acetone: A Tracer for Concentration Measurements in Gaseous Flows by Planar Laser-Induced Fluorescence," *Experiments in Fluids*, Vol. 13, 1992, pp. 369–376.

Modular Ignition System Based on Resonance Igniter

M. Niwa,* A. Santana Jr.,† and K. Kessaev‡

Instituto de Aeronáutica e Espaço,

12228-610 São José dos Campos/SP, Brazil

Introduction

FURTHER space exploration is centered on rocket engines that operate with powerful propellants based on oxygen. Because propellant combinations involving oxygen are nonhypergolic, the provision of engines by a simple and reliable ignition system is one of several topical problems. Additionally, where engines for upper stage and space system applications are concerned, the introduction of an ignition system with the possibility of multiple starts is also fundamental.[1]

In liquid-oxygen (LOX)-based engines ignition is usually realized through a torch, where spark ignition is considered as the most suitable for multiple starts. However, it is provided at the cost of large amounts of hardware for two independent subsystems fluid and electrical, and hence assurance of the system reliability is not an easy task. In 1970 Phillips et al.[2] produced a torch igniting a gaseous oxygen–hydrogen mixture inside a resonance tube (resonance ignition). By that time it was known that a gas jet accelerated through a sonic nozzle could provoke inside a deep cavity (resonator) shock-wave oscillations with heat release sufficient to ignite propellant mixtures.[3–5]

The resonance ignition is attractive because of the extremely simple configuration and possibility of multiple ignitions. However, operating the ignition system with gaseous hydrogen (GH_2) is coupled

Received 13 December 2000; revision received 20 April 2001; accepted for publication 2 June 2001.

*Head of Propulsion Division; niwa@iae.cta.br. Member AIAA.

†Research Engineer; santanajr@iae.cta.br.

‡Visiting Researcher; kessaev@iae.cta.br.